HHS Public Access

Author manuscript

J Colloid Interface Sci. Author manuscript; available in PMC 2020 September 15.

Published in final edited form as:

J Colloid Interface Sci. 2019 September 15; 552: 689–700. doi:10.1016/j.jcis.2019.05.071.

Magnetic liposome design for drug release systems responsive to super-low frequency alternating current magnetic field (AC MF)

Kseniya Yu. Vlasova[†,1], **Alexander Piroyan**[†,2], **Irina M. Le-Deygen**[1], **Hemant M. Vishwasrao**[2], **Jacob D. Ramsey**[2], **Natalia L. Klyachko**[1,2,3], **Yuri I. Golovin**[1,3], **Polina G. Rudakovskaya**[1], **Igor I. Kireev**[4], **Alexander V. Kabanov**[1,2,*], **Marina Sokolsky-Papkov**[2,*]

[1]Laboratory of Chemical Design of Bionanomaterials, Faculty of Chemistry, Lomonosov Moscow State University, Moscow, 119992, Russia

[2]Center for Nanotechnology in Drug Delivery and Division of Pharmacoengineering and Molecular Pharmaceutics, Eshelman School of Pharmacy, University of North Carolina at Chapel Hill, NC 27599, U.S.A.

[3]G.R. Derzhavin Tambov State University, Tambov, 392000, Russia

[4]A.N. Belozersky Institute of Physico-Chemical Biology, M.V. Lomonosov Moscow State University, Moscow, 119992, Russia

Abstract

Hypothesis—Magnetic liposomes are shown to release the entrapped dye once modulated by low frequency AC MF. The mechanism and effectiveness of MF application should depend on lipid composition, magnetic nanoparticles (MNPs) properties, temperature and field parameters.

Experiments—The study was performed using liposomes of various lipid composition and embedded hydrophobic MNPs. The liposomes structural changes were studied by the transmission electron microscopy (TEM) and attenuated total reflection Fourier transfer infrared (ATR-FTIR) spectroscopy and the leakage was monitored by the fluorescent dye release.

Findings—Magnetic liposomes exposure to the AC MF resulted in the clustering of the MNPs in the membranes and disruption of the lipid packaging. Addition of cholesterol diminished the dye release from the saturated lipid-based liposomes. Replacement of the saturated lipid for unsaturated one also decreased the dye release. The dye release depended on the strength, but not the frequency of the field. Thus, the oscillating motion of MNPs in AC MF ruptures the gel phase membranes of saturated lipids. As the temperature increases the disruption also increases. In the

[*]Corresponding authors: kabanov@email.unc.edu, msokolsk@email.unc.edu.
[†]Authors contributed equally to this work.

Conflicts of interest
There are no conflicts to declare.

liquid crystalline membranes formed by unsaturated lipids the deformations and defects created by mechanical motion of the MNPs are more likely to heal and results in decreased release.

Keywords

magnetic liposomes; lipid composition; drug release; super-low frequency AC MF

Introduction

In recent decades the investigation of nanoscale containers for targeted delivery and controlled release of therapeutic agents has become a top priority in pharmaceutical science and drug development [1–4]. Liposomes are one of the best studied types of such containers that have been used in several dozens of marketed products. The Food and Drug Administration (FDA) approved liposomes are characterized by high stability, long circulation time and low leakage of encapsulated drug molecules, which are all important for successful delivery of the drugs to target sites, such as tumors. However, numerous studies have also attempted to increase the release rate of the drugs from liposomes in the target site. Many factors (such as temperature [5] or lipid composition [6]) affect membrane diffusion of solutes due to formation of defects in the lipid bilayers. Thus, lipid vesicles sensitive to intrinsic (e.g., lower interstitial pH in tumors or higher glutathione concentration in cells) [7] or externally applied stimuli (e.g., light, ultrasound, magnetic and electric fields) [8] were studied.

The use of magnetic fields has some significant advantages compared to other external stimuli. One heavily explored area in this regard is the magnetic hyperthermia. Thermosensitive liposomes, conjugated to single-domain magnetic nanoparticles (MNPs) incorporated into lipid bilayer or water pool of the liposome, have increased permeability under exposures to high frequency AC MF [9–14]. The field-induced release of solutes from such magnetic liposomes is based on the Brown and Neel relaxation phenomena [15]. It is believed that the field interaction with MNPs leads to a heat generation that can increase the temperature of the lipid bilayer above the phase transition temperature (Tm) and produce the drug release effect [16]. The limitations of such approach include a rapid heat dissipation in the surroundings decreasing the temperature gradients, a need of using high concentrations of MNPs in liposomes to reach the Tm and a potential of heat induced injury of the healthy tissues.

Thus, a potential of controlled release of solutes from magnetic liposomes using “non-heating” low frequency AC MF has attracted growing interest. This approach, called “magneto-mechanical actuation”, involves generation of mechanical forces by single-domain MNPs that undergo oscillating movement in low frequency AC MF [17]. The magneto-mechanical actuation has been shown to affect functions of various biological systems (cells, enzymes, Na/K channel, etc.) [18–20]. One of the main advantages of such approach is the relative safety of the low frequency AC MF to human body and the localized affect upon targeted magnetic liposomes. The studies on the dye or drug release from various magnetic liposomes reported increased permeability of such liposomes observed upon application of low frequency AC MF [21–24]. Despite the initial promise of the studies

using this approach the underlying physical and molecular mechanisms are not entirely clear and the principles for optimizing the container structure and field parameters have not been fully established. Our previous works [17, 25] described the theoretical studies on the magneto-mechanical actuation of different nanosystems (including lipid membranes) by low frequency AC MF through single-domain MNPs. The field effects in such systems depend on a variety of factors such as MNPs design, nature of MNPs microenvironment, and field characteristics.

Here we explored the processes occurring in magnetic liposomes of various lipid compositions (saturated or unsaturated lipids, cholesterol (Chol), PEGylated and non-PEGylated lipids) with small hydrophobic iron oxide MNPs (5 or 7 nm in diameter) within the membrane after exposure to non-heating low frequency AC MF. The aim of this study is to understand the phenomena of the dye release from the magnetic liposomes and provide rationale for design of such liposomes for future applications.

Materials and Methods

Materials

Phospholipids, 1,2-Distearoyl-sn-glycero-3-phosphotydilcholine (DSPC), egg L-α-phosphocholine (eggPC), Chol and 1,2-distearoyl-sn-glycero-3-phosphoethanol-amine-N-[methoxy-(polyethylene glycol)-2000] ammonium salt (DSPE-PEG2000) were purchased from Avanti Polar Lipids, Alabaster, AL. Iron (III) acetylacetonate ($Fe(acac)_3$), benzyl alcohol (anhydrous), 6-nitro-dopamine hydrogen sulfate, N-(palmitoyloxy)succinimide (palmitoyl-NHS), calcein, carboxyfluorescein (CF), triethylamine, nitric acid (TracesELECT), hydrochloric acid (TraceSELECT), inductively coupled plasma mass spectrometry (ICP-MS) grade standards for Iron (Fe) and Phosphorus (P) (Fluka) were purchased from Sigma-Aldrich (St. Louis, MO). All chemicals were analytical grade and were used as received. Acetone (histology grade), ethanol and all other anhydrous high-performance liquid chromatography (HPLC) grade organic solvents were purchased from Thermo Fisher Scientific (Waltham, MA).

Synthesis and characterization of iron oxide MNPs

MNPs were synthesized by thermal decomposition of $Fe(acac)_3$ in benzyl alcohol [26]. Briefly, 4 μmoles of $Fe(acac)_3$ was charged to a three-necked flask containing 20 ml anhydrous benzyl alcohol. The synthesis was conducted under inert atmosphere. To produce ~5-6 nm MNPs the reaction mixture was heated at 70°C for 1 h, then the temperature was gradually increased at 0.4°C/min to 150°C, and then kept constant for 24 h. Alternatively, to produce ~7-10 nm MNPs after 1 h incubation at 100°C, then the temperature was increased at 0.4°C/min to 210°C, and then kept constant for 40 h. In both cases after cooling, the MNPs were precipitated and washed in acetone. The final product was collected by magnetic separation, dried under vacuum and stored for further use under vacuum in a sealed vial filled with argon. The MNPs were characterized by Mössbauer spectra, Transmission electron microscopy (TEM) and the saturation magnetization (Supplementary Figures S1, S2).

Synthesis and characterization of N-palmitoyl 6-nitro-dopamine (PNDA)

PNDA was synthesized using a modified procedure from the reference [16] (Amstad et al.). Briefly, 64.3 mg 6-nitro-dopamine hydrogen sulfate and 51.2 mg of palmitoyl-NHS (molar ratio 1.5:1.0) were dissolved in 0.5 ml dimethylformamide (DMF) and supplemented with 0.1 ml triethylamine. The solution was stirred at room temperature (r.t.) for 20 h under nitrogen atmosphere. The reaction mixture was acidified with concentrated hydrochloric acid, the product was precipitated by deionized (Dl) water (Millipore), washed several times with Dl water, methanol and finally ethyl ether and dried under vacuum. The structure and purity of the product were confirmed by **^{1}H NMR**. The yield of the reaction was ~60%.

MNPs coating with PNDA

MNPs were coated with PNDA as previously described in the reference [16] (Amstad et al.). Briefly, 6 mg PNDA was dissolved in 60 μl DMF and then diluted with 0.5 ml ethanol. The resulting solution was added to 1 mg of the freshly synthesized (~2 h) MNPs dispersed in 0.5 ml ethanol. The mixture was stirred at 50°C for 24 h, and then the PNDA-coated MNPs were separated with a magnet, washed three times with 1 ml of ethanol, re-dispersed in 1 ml of Dl water and lyophilized to dryness. The PNDA content in the PNDA-MNPs was ~20% w/w as determined by thermogravimetric analysis (TGA) (Supplementary Figure S3). Packing density of of PNDA on the MNP surface was calculated as

$$PD = \frac{4 \cdot \pi \cdot R_{MNP}^{3} \cdot \%(PNDA) \cdot N_A \cdot \cdot \rho_{MNP}}{3 \cdot \%(MNPs) \cdot M_{PNDA}},$$

where R_{MNP}: MNP radius, N_A: Avogadro constant, ρMNP: magnetite density, M_{PNDA}: PNDA molecular weight.

Preparation of liposomes

Liposomes were prepared by reverse phase evaporation method using two basic variations. A). Two milligrams (2 mg) of DSPC or eggPC were mixed with DSPE-PEG2000 (and in selected cases Chol), supplemented with PNDA-MNPs (1 mg, 0.5 mg or 0.2 mg) and dispersed in 6 ml of chloroform:diisopropyl ether mixture (1:1). B). Alternatively, 10.5 mg eggPC were mixed with 0.7 mg Chol (and in selected cases DSPE-PEG2000) and supplemented with 0.1 mg of bare MNPs in 1 ml of chloroform. The mixtures A or B were sonicated until fully dispersed and then incubated at r.t. in a shaker for 30 min prior to adding 1 ml of 5 mM calcein solution in 10 mM phosphate-buffered saline (PBS), pH 7.4 (A) or 0.33 ml of 50 mM CF solution in 10 mM PBS, pH 7.4. The mixtures were intensively vortexed and bath sonicated to form stable emulsion. The organic solvents were evaporated on a rotary evaporator until almost clear aqueous dispersion of liposomes was formed. The volume of the dispersion was adjusted to 1 ml by addition of 10 mM PBS, pH 7.4 or Dl water and the dispersion was vortexed and bath-sonicated until formation of a clear solution. Liposomes were sequentially extruded through 400 nm and 200 nm polycarbonate filters (10 times through each filter, in selected cases 20 times just through the 200 nm filter) at 25°C (most eggPC-based systems) or 65°C (all DSPC based systems) using a hand extruder (Avanti, Arab, AL). The unincorporated dyes were removed by gel filtration on Sepharose

CL-4B column (A) or NAP-25 column (B). The calcein and CF loaded liposomes were used within 24 h or 5-6 h after preparation. The MNPs content was quantified by Iron (Fe) using ICP-MS or Inductively coupled plasma atomic emission spectrometry (ICP-AES) and the phospholipid content was quantified by Phosphorus (P) using ICP-MS as described in the Supplementary methods. The composition of liposomes used in this work is summarized in the Table 1.

Characterization of liposomes

The average mean particle diameters (D_{ave}) were determined by nanoparticles tracking analysis (NTA) using Nanosight NS500 (Malvern Instruments, MA, USA). The z-average hydrodynamic diameter (D_{eff}), polydispersity index (PDI) and ζ-potential were determined by dynamic light scattering (DLS) using a Malvern Zetasizer Nano ZS (Malvern Instruments, MA, USA). TEM images were taken on a JEOL 2010F-FasTEM HRTEM (Peabody, MA). Briefly, samples were diluted to approximately 0.2 mg/ml in Dl water. A 5-10 μl sample was placed on a copper TEM grid coated with carbon support films (Tedpella INC, Redding, CA) and allowed to settle for 1-2 min. The excess sample was carefully removed and the grid was allowed to dry for another 5-10 min. Next, the grid was covered with a small drop of 2 % uranyl acetate, allowed to settle for 0.5-1 min, excess of the staining was removed and the sample was analyzed by TEM. Atomic force microscopy (AFM) and Magnetic force microscopy (MFM) were carried out using Solver Next NT-MDT spectrum instrument (Zelenograd, Russia) as detailed in the Supplementary information. The melting temperatures of the liposomal membranes were determined by the differential scanning calorimetry (DSC) using a VP-DSC calorimeter (MicroCal, GE Healthcare, Freiburg, Germany) at a heating rate of 60°C/h. Fourier-transform infrared (FTIR) spectra were recorded using a Bruker Tensor 27 spectrometer equipped with a liquid nitrogen cooled mercury cadmium telluride (MCT) detector. Samples were placed in a thermostated cell BioATR-II with a ZnSe attenuated total reflection (ATR) element (Bruker). The FTIR spectrometer was purged with a constant flow of dry air. FTIR spectra were acquired from 900 to 3000 cm^{-1} with 1 cm^{-1} spectral resolution. For each spectrum, 100 scans were accumulated at 20 kHz scanning speed and averaged. All samples were prepared in aqueous buffer solution using deionized water at 22°C. Spectral data were processed using the Bruker software Opus 7.5, which includes linear blank subtraction, straight-line baseline correction and atmosphere compensation. If necessary, seven- or nine-point Savitsky-Golay smoothing was used to remove white noise. Peaks were identified by standard Bruker picking-peak procedure.

Calcein release from liposomes

The stability of liposomes was evaluated by incubating the samples in 10 mM PBS (pH 7.4) at 4°C or 40 mg/ml fetal bovine serum (FBS) in 10 mM PBS (pH 7.4) at 37°C. Briefly, liposomes at concentration of 0.08 mg lipid/ml were placed in Float-a-lyzer© dialysis membrane tubes (3.5 – 5 kDa MWCO; 1 ml capacity; Spectrum Labs, USA). The volume in the tubes was adjusted to 1 ml, the assembly was placed in a 24 ml dissolution medium and stirred at approximately 125 rpm for 24 h. At specific time points during the study, 0.5 ml aliquots were removed from the dissolution medium outside the dialysis membrane and replaced with same volume of the fresh buffer. The fluorescence intensity of calcein in the

dissolution medium was measured using NanoDrop-3000 (Thermo Fischer, excitation 495, cut off 515, emission 525 nm), quantified and plotted vs. time.

Exposure to Magnetic Field

The super-low frequency AC MF generator was custom designed and purchased from Nanomaterials Ltd. (Tambov, Russia). The unit contains a sinusoidal current generator with variable power (up to 1.5 kW), frequency (in the range from 30 to 3000 Hz) and variable magnetic field amplitude (from 10 to 160 kA/m). The unit is equipped with a water-cooled inductor with a ferromagnetic core and a temperature-controlled exposure chamber. The temperature-controlled samples holder accommodates one 8-well strip plate at a time, allowing concurrent replicates evaluations. Field frequency and field intensity were measured and monitored by an oscilloscope throughout the application time. For the MF exposure experiments, the M-LPS samples were used as prepared (in selected cases at 5-fold dilution or 10-fold dilution in PBS), and exposed to MF as specified. The release from calcein-loaded liposomes was observed in situ. To observe the release from CF-loaded liposomes, 500 μl of the sample was placed into dialysis membrane (cut-off 10 kDa). The dialysis membrane was sealed and immersed in 10 ml of PBS (10 mM, pH 7.4) and aliquots of PBS were collected at 5 min time interval. The fluorescence of the released calcein was measured using NanoDrop-3000 (Thermo Fischer, excitation 495, cut off 515, emission 525 nm). The fluorescence of the released CF was measured using SpectraMax M5 (Molecular Devices, excitation 475, cut off 505, emission 515 nm).

The percentage of released dye was calculated as following:

$$\%\ Release = 100 * \frac{\left(F_t - F_0\right)}{\left(F_{100} - F_0\right)},$$

where F_0 is the fluorescence measured at t_0; F_t is the fluorescence at specific time point t; and F_{100} is the total released fluorescence. The F_{10}o value was obtained by lysing the M-LPS with 1% Triton X-100 to destroy the liposomal structure and release the total incorporated dye. MNP free dye-loaded liposomes of the same compositions were used in all experiments as magnetite-free controls.

Statistical Analysis

Statistical analyses were performed using GraphPad Prism (GraphPad Software, Inc, La Jolla, CA). ANOVA or two-tailed Student's t-tests was used to analyze data. Where applicable, reported p-values have been adjusted for multiple comparisons using the Ryan-Einot-Gabriel-Welsch post-hoc method. Significance was reported for $p<0.05$.

Results

The bare MNPs with the average diameter of ~5-6 nm or ~7-10 nm were prepared by thermal decomposition of $Fe(acac)_3$ in benzyl alcohol. The larger MNPs were mainly magnetite (Fe_3O_4) while the smaller ones contained relatively higher content of maghemite (Fe_2O_3) as determined by Mössbauer spectrometry (Supplementary Figures S1, S2). MNPs

were coated with either PNDA (through nitrodopamine group) or eggPC (through charged headgroup of eggPC). Based on TGA data (Supplementary Figure S3), the density of coating of PNDA/MNPs was 130 units/particle or 1.6 PNDA/nm^2.

As a result, the MNPs acquired a hydrophobic exterior layer that enabled their incorporation into the inner hydrophobic area of a liposome membrane. We varied the liposome lipid composition as presented in Table 1 by adding Chol that affects the membrane fluidity and DSPE-PEG2000 to assess the effect of PEG coating in PEGylated vs non-PEGylated liposomes. Overall, for the PEGylated liposomes variation of the lipid composition did not affect the hydrodynamic diameter (D_{eff} ~ 100-105 nm), and polydispersity (PDI ~ 0.11-0.14). All PEGylated liposome particles were nearly neutral (ζ-potential ~ - 3.2 - 4.2 mV). However, in the absence of DSPE-PEG2000 the formed non-PEGylated liposomes were considerably larger (D_{eff} ~ 150 nm) and displayed a negative charge (ζ-potential - 12.7 mV). There appeared to be also a dependence of the liposome size on the size of the MNP – as the magnetite grain increased from 5 to 7 nm both the PEGylated and non-PEGylated liposomes became larger (Table 1). The incorporation of the MNPs into the liposomes was visualized by TEM (Figure 1A, Supplementary Figure S6) as well as AFM and MFM analysis (Supplementary Figure S7). TEM clearly reveals electron-dense MNP grains inserted in liposomes, while AFM and MFM analysis can distinguish magnetite-free and magnetite-containing liposomes for relatively low MNPs concentrations. The extent of incorporation of MNPs in the liposomes depended on the lipids/MNP feed ratio used for preparation of the liposomes and at some point “overloading” of the lipids by the MNPs did not help incorporation. As the feed of MNPs relative to lipids increases, the lipid coated MNPs are likely to aggregate with each other rather than interact with lipids and uniformly distribute into lipid membranes. Since the lipid membranes can not incorporate MNPs larger than 5nm in diameter without membrane disruption, the aggregation of MNPs is a likely reason for their reduced incorporation into liposomes at the higher MNPs to lipid feed ratio. Generally, the less the MNP was added to the lipids the more MNP was incorporated (Supplementary Table S1). Replacement of DSPC for eggPC for the same lipid/MNP ratio did not seem to change the MNP incorporation considerably although addition of Chol had somewhat more profound effect (Supplementary Table S2).

To confirm the closed vesicular structure of the liposomes they were loaded with a self-quenching fluorescent dye, calcein. After treatment with 1% Triton X-100 the fluorescence increased due to calcein release from the liposome aqueous pool, and the fluorescence changes indicated that the sizes of this pool for the MNP-free and MNP-containing liposomes were approximately equal (Figure 1B). After Triton X-100 treatment liposomes also displayed a change of the z-average hydrodynamic diameter from ~100 nm to ~30 nm as confirmed by DLS, which was consistent with the formation of lipid-surfactant micellar aggregates (Figure 1C). All liposome samples with different MNP content displayed the closed lipid vesicle structure and entrapped approximately same amount of calcein (Supplementary Figure S9).

Both MNP-containing and MNP-free liposomes were stable upon storage at **4°C** for at least 24 h (Figure 1D). However, at **37°C** in presence of FBS MNP-free liposomes released calcein nearly entirely. In contrast, under these conditions MNP-containing liposomes

appeared to be less leaky as they released less than 25% calcein (Figure 1D). Interestingly, the presence of MNPs within the lipid bilayer has been previously associated with the membranes stiffening [27], which may decrease fusion of the MNP-containing liposomes and explain their elevated stability upon storage in the presence of FBS. Incorporation of the MNPs into the liposomal membrane increased the melting point of the phospholipids by about 1 degree as confirmed by DSC (Figure 1E).

In the experiments involving the effects of the AC MF on the magnetic liposomes we first examined the stability of the liposomes by measuring the particle sizes before and after the field application at 25°C or 37°C. For the PEGylated DSPC/DSPE-PEG2000 MNP-liposomes (that are below the phase transition temperature) or eggPC/DSPE-PEG2000/Chol MNP-liposomes (that are above the phase transition temperature) there were little if any changes in the particle size (less than 10 %) (Table 2, Supplementary Tables S3, S4). However, the size of the non-PEGylated eggPC/Chol MNP-liposomes increased considerably during the treatment (Table 2) and did not restore to the original value when the field was switched off (Supplementary Table S6). To better understand the structural transitions proceeding in the magnetic liposomes we performed TEM imaging before and after application of the magnetic field (Figure 2). Within the first few minutes of exposure to the AC MF the MNP grains appeared to become more clustered within the membranes of both non-PEGylated and PEGylated liposomes (Figure 2, compare panels A, D, G and B, E, H). In selected cases there appears to be several liposomes assembled together by the islands of their MNP grains, which is most distinct in the case of the PEGylated liposomes. Further exposure revealed the differences in the behavior of these liposomes. The non-PEGylated ones became destructed and aggregated, with the large and shapeless clusters of magnetite becoming prominent and lipid vesicles practically indistinguishable after 25 min of the exposure (Figure 2C). The PEGylated liposomes appear to reveal some remaining lipid membrane structures with the clustered magnetic nanoparticles albeit become more aggregated with multiple liposomes coming together (Figure 2F, 2I). In comparison in the direct current (DC) field of a similar strength already after 5 min the PEGylated liposomes appear to align into large spindle-like (columnar) structures (Figure 2J).

To probe the fine structure of the lipid bilayer in the magnetic liposomes we used ATR-FTIR spectroscopy. As expected, comparison of the ATR-FTIR spectra reveals no changes for the MNP-free non-PEGylated and PEGylated liposomes suggesting that addition of the PEG chains at the surface of the bilayers does not affect the arrangement of the lipid molecules (Figure 3A, Supplementary Figure S10A). At the same time incorporation of the MNPs in the liposomal membranes results in alteration in the most intense absorption band corresponding to asymmetric stretching vibrations of CH_2 groups (CH_2as) (2923 cm^{-1}) (Figure 3B, Supplementary Figure S10B). The observed high-frequency shift of this band is consistent with an increase in the mobility of the hydrocarbon chains and lipid membrane fluidity [28]. Additionally, the changes in the intensity of the absorption bands of the carbonyl group (1730-1740 cm^{-1}) and the low frequency shift in the asymmetric oscillations of phosphate group, PO_2^-as (from 1227 to 1222 cm^{-1}), suggest that incorporation of MNPs in the liposomes result in the microenvironment changes and hydration of the phosphate head groups at the lipid-water interface [29]. Following exposure of the magnetic liposomes to the AC MF there were further changes in the position of the CH_2as band. Specifically, for

both non-PEGylated and PEGylated magnetic liposomes containing 5 nm MNP the band maximum shifted to lower frequencies suggesting dehydration and increase in the packing density of the hydrocarbon chains (Figure 4). The changes in the bands corresponding to the carbonyl and phosphate group were more difficult to interpret although somewhat more pronounced high frequency shift in the PO_2^-as band observed for PEGylated magnetic liposomes may suggest increased dehydration of the phosphate head groups (Supplementary Figure S11). Surprisingly for PEGylated magnetic liposomes containing 7 nm MNPs after exposure to the field produced a high-frequency shift in CH_2as suggesting an increase in the alkyl chains mobility along with an increase of the shoulder in the band of non-hydrogen bonded carbonyl group (1740 cm^{-1}) (Supplementary Figure S12). This could be due to different localization of the MNPs in the lipid membranes due to the difference in the MNP sizes. In all cases the absorption bands corresponding to symmetric stretching vibrations of CH_2 groups (CH_2s) (2850 cm^{-1}) appeared to be unaffected.

Next, we examined effects of AC MF on the integrity of the membranes of the magnetic liposomes as assessed by the release of the entrapped dyes (calcein, CF). In all cases we observed that the exposure to the field resulted in the release of the dyes from the magnetic liposomes (Figure 5, Supplementary Figure S13). No field-induced release of the dye was observed from the MNP-free liposomes. The dye release from the magnetic liposomes displayed some dependence on the field parameters (Figure 5, Supplementary Figure S14). No significant difference in the calcein release was observed between 50 Hz and 350 kHz, at the field strength of 30 kA/m. However, at higher field strength of 50 kA/m the extent of the dye release was increased, albeit above this point the effects of the field appeared to level-off. The estimated theoretical critical frequency, ω_c, above which the angular velocity of the particle cannot increase, is approx. 65 Hz for our particular DSPC-containing system (see, Supplementary information). That means, that further increase of the frequency (above 65 Hz) of the external field leads to saturation and even decrease of the amplitude of the particle oscillations and, as a result, to the decrease of potential deformations of the lipid bilayer in the immediate vicinity of the MNPs. As the temperature increased from 25°C to 37°C the field-induced dye release also increased. However, this temperature effect was not associated with the phase transition in the bulk of the lipid bilayer since both tested temperatures were lower than the bilayer melting point (54°C) (Figure 1E). To examine whether the release of the dye was due to its temperature-induced mobility, we exposed M-LPS to RF field at 32°C (Supplementary Figure S15). The release of the dye under these conditions was not much higher than that observed with the M-LPS at 25°C. This data is supportive of the proposed magneto-mechanical mechanism of the release, as we would expect a linear dependence of the dye diffusion across the membrane and its release on the temperature. Notably, exposure of the magnetic liposomes to the DC MF of equal strength did not produce any measurable calcein release at either temperature.

To examine how the duration of the field exposure affects the calcein release the magnetic liposomes were exposed to 50 kA/m, 50 Hz field at 37°C for different times up to 40 min. The amount of the probe released increased from zero to about 80% as the duration of the exposure increased up to 30 min, and then remained unchanged (Figure 6A). Notably, no additional calcein release was seen with the samples exposed to the field or 20 min and then incubated for up to 24 h without the field (Figure 6B). This suggests that the membrane

permeabilization is induced directly by and during continuous exposure of the magnetic liposomes to the field but is does not last after the field exposure. No difference in the calcein release was observed between the continuous and pulsed (on-off-on…) regimes of the magnetic liposomes exposure to AC MF. Specifically, the release of the probe was the same for 1) 30 min continuous exposure to AC MF (50kA/m, 50Hz); 2) 3 × 10 min MF exposures with 5 min intervals, and 3) 6 × 5 min MF exposures with 0.5 min intervals (Supplementary Figure S16).

To assess whether the release of the calcein in AC MF could be affected by the lipid composition of the magnetic liposomes the latter were prepared using saturated lipids mixture DSPC/DSPE-PEG2000 or unsaturated lipids mixture eggPC/DSPE-PEG2000 each with or without added Chol (Table 1). All resulting magnetic liposomes had very similar particle hydrodynamic diameters (D_{eff} ~100 nm to ~ 104 nm, PDI ~ 0.12 – 0.14) and charge (ζ-potential ~ - 3.2 mV to - 4.2 mV). Albeit there was ~1.6-fold difference in the MNP content between the saturated and unsaturated lipid based compositions addition of Chol did not change the amount of the MNP incorporated in each of these formulations. The structure of the magnetic liposomes was confirmed by TEM (Supplementary Figure S6). Each liposome formulation incorporated and released after adding Triton X-100 approximately the same amount of calcein (Supplementary Figure S17). These magnetic liposomes were exposed for 30 min to 50kA/m, 50Flz AC MF at 25°C and 37°C (Figure 7). Replacing DSPC for eggPC greatly diminished the field-induced release of the probe at both temperatures (Figure 7A). There was also a dramatic decrease of the calcein release in the magnetic liposomes containing Chol compared to the Chol-free liposomes (Figure 7B) [30]. No field-induced release of the dye was observed from the corresponding MNP-free liposomes. Both PEGylated and non-PEGyalted liposomes accelerated the release of the dye under the AC MF albeit the PEGylation slightly decreased the release under the similar conditions (Supplementary Figure S12). Quite unexpectedly, we discovered that the concentration of the magnetic liposomes in the dispersion had a profound effect on the extent of caclein release after liposomes exposure to the field. Specifically, as the magnetic liposomes concentration decreased, the relative calcein fluorescence after AC MF exposure became greater (Figure 8). This effect was noticeable at 25°C, but was much stronger at 37°C. Thus, at 25°C magnetic liposomes released ~ 11% of calcein at 0.8 mg lipid/ml, ~20% at 0.16 mg lipid/ml, and ~ 29% at 0.08 mg lipid/ml (Figure 8A). At 37°C the same magnetic liposomes released ~ 20%, ~60%, and ~80% of calcein, respectively (Figure 8B). Since the liposome concentration should define the total concentration of calcein in the solution we evaluated whether the observed dependence could be due the probe self-quenching. For this purpose, magnetic liposomes were disrupted by 1% Triton X-100 in the absence of the AC MF. As the liposome concentration decreased from 0.8 mg lipid/ml to 0.08% the resulting relative fluorescence of calcein slightly increased (Supplementary Figure S18). This is probably due to attenuation of the probe self-quenching upon decrease of the liposome (and probe) concentration. Notably, the liposome disruption by Triton X-100 releases calcein entirely. However, the magnitude of the fluorescence changes (not more than about 1.3-fold at 0.08 mg lipid/ml) was insignificant when compared to the differences observed in the AC MF experiments. Therefore, the extent of liposome leakage upon exposure to AC MF indeed increased as the liposome concentration decreased. At the same time the MNPs-MNPs

interactions within the lipid membrane did not seem to play a significant role in the probe releases from liposomes (Figure 8). The only exception was observed at 0.16 mg lipid/ml at 37°C where the probe release changed from ~33% to ~53% as the MNP content in the liposomes increased from 5.5% to 10% w/w. However, these changes were small compared to those observed upon the changes in the liposomes concentration.

Discussion

The phenomenon of a solute release from magnetic liposomes induced by a low frequency AC MF was first described by Nappini et al. who used for this purpose hydrophobic (oleic acid-stabilized) or hydrophilic (citrate-stabilized) $CoFe_2O_4$ nanoparticles incorporated in the liposome membrane or aqueous pool [21, 31]. The release of a dye (CF) from both types of systems was observed following exposure to AC MF for 10 to 50 min. Subsequent works explored liposomes of various lipid compositions with MNPs incorporated within the lipid bilayer or attached to its inner or outer surface [22–23]. These various structures were all shown to release entrapped fluorescent dyes or drug molecules in response to the field exposures, albeit the release proceeded at varying rates and to different extents depending on the used field parameters and liposome and MNPs compositions. The membrane permeability increases in the AC MF were ascribed to changes in the lipid membrane structure that were assumed, but never directly demonstrated. Of significance therefore is that our study indeed confirms perturbations in lipid packaging by ATR-FTIR spectroscopy after the exposure of the magnetic liposomes to the AC MF. Noteworthy, the use of an alternating field is essential since the magnetic liposomes do not release the solutes in the DC fields of similar strength as shown in our work. This suggests that clustering of MNPs within the lipid membrane as a result of magnetization and alignment of the MNPs magnetic moments (that proceeds in either DC or AC MF) alone cannot explain the solute release effect.

Few studies discussed the physical mechanism of the process. Suggested explanations can be grouped into two distinct mechanisms involving either 1) mechanical or 2) thermal effects of MNPs upon the lipid bilayer. For example, Qiu and An implied that the AC MF produces both MNPs oscillating movements and heat generation that combined induce transition of the liposomal membrane to a liquid crystalline state [23]. Shaghasemi et all suggested that the local temperature increase in the membranes of magnetic liposomes after their exposure to a pulsed AC RF field (75kA/m, 228KHz, 3 min “on”, 5min “off”) induces defects in the membrane separating melted liquid and solid gel domains and results in the release of the loaded calcein without causing damage to the membrane structure (as confirmed by lack of calcein leakage after the field withdrawal) [32]. Chen et all demonstrated changes in membrane structures, specifically fusion and formation of bilayer sheets following exposure of magnetic liposomes to RF heating at 250 A and 281 kHz for 2400 sec. The proposed mechanism suggested that nanoparticles or nanoparticle aggregates within the bilayer led to the fusion of neighboring or concentric magnetic liposomes [33]. These differences are likely due to longer duration of field exposure (20 min). However, estimates suggest that the local or system-wide heating created by the interaction of AC MF with MNPs is negligible for the relatively “weak” low frequency fields (e.g. $f < 1$ kHz, $H < 100$ kA/m) [17]. As a result several authors raised doubts about the thermal mechanism. For example, Spera et al.

[34] deliberately used magnetic liposomes with the phase transition temperature greatly exceeding the ambient temperature in order to exclude the thermal mechanism. They observed the release of CF under AC MF in the continuous and pulsed modes and ascribed it to a mechanical destabilization of the bilayer by MNPs.

The low frequency AC MF can produce oscillating rotational–vibrational movement of the single-domain MNPs embedded in the lipid bilayer [17]. The torque and deformations as a result of such movement can perturb the local lipid packaging or even rupture of liposomal membranes. The stiffening of the membrane by the embedded MNPs (as determined by an increase in Young's modulus) along with the membrane morphological inhomogeneity makes the membrane more susceptible to the mechanical rupture in the AC MF by the vibrating MNPs [27]. A detailed consideration of the magneto-mechanical effects of MNPs in lipid membranes including estimates of mechanical forces and deformations generated by oscillating MNPs are found in reference [17] (Golovin et al.). These effects depend on a variety of factors such as MNPs design (e.g. material, size, mass, and shape), nature of lipid microenvironment (viscosity, elasticity and relaxation behavior), and field characteristics (spatial distribution, amplitude, frequency, variation of the field orientation). In particular, the forces were predicted to increase as the field strength increases but remain relatively constant as the frequency increases. Consistent with this prediction we observed here a dependence of the dye release from the magnetic liposomes on the strength but not on the frequency of the field. The rapid formation of the clusters of the MNPs within the lipid membrane after application of the AC MF can enhance the effects of the embedded MNPs as the forces generated by them were shown to be greater for larger and anisotropic (e.g. rod) structures (Scheme 1) [17,25].

Noteworthy, in our studied systems the dye release was continuous and concurrent with the application of the AC MF (Figure 6). It levelled off at ca. 30-40 min, presumably due to exhaustion of the magnetic liposome fraction in the overall liposome population. When the field exposure was interrupted before the completion of the release no further release (post field) was observed. This seems to be similar to the report by Bi et al. [22] that the encapsulated molecules are released from the magnetic liposomes only during the field exposure. Some other studies reported a non-monotonous dependence of the dye release after the field application, for example, a low leakage during first several hours followed by a delayed massive release from non-PEGylated unsaturated lipid liposomes with the oleic acid coated $CoFe_2O_4$ MNPs [21, 31].

In this context it is of interest that we discovered that the dye release could depend on the liposome-liposome interactions. In our case the release was inhibited as the liposomal concentration increased. Although, we did not observe a strong dependence of the particle size on the liposome concentration in the absence of AC MF, a transient aggregation of the magnetic liposomes during the field exposure is possible [35–36]. Such aggregation may be facilitated by the alignment of the magnetic moments of the MNPs across different liposomes. The observed concentration "inhibition" of the probe release may be due to a self-assembly of liposomes, which could either 1) slow-down the concerted motion of the MNPs and lipid membranes in the oscillating field and thereby inhibit the lipid bilayer

rupture, or 2) decrease the effective area of contact of the perturbed lipid bilayer sites with the external solution instead enabling the passage of the dye from one liposome to another.

Therefore, the resulting release behavior in the magnetic liposomes may strongly depend on their composition. In the present work we explored the design parameters that could be important for the development of remotely actuated liposomal drug release systems involving magneto-mechanically controlled lipid membrane permeability and release of the entrapped solutes. Accounting for the need of translating the results to biomedical applications we chose iron oxide MNPs as a biocompatible material [37], and evaluated the role of the liposome surface PEGylation and the lipid membrane composition that are essential factors for manufacturing of the magnetic liposomes stable in biological environments.

First, we examined two different iron oxide MNP systems of 5 nm and 7 nm in diameter and concluded that the loading of these particles in magnetic liposomes was different – a greater amount of 5 nm MNPs incorporated in the lipid bilayer compared to 7 nm MNPs. This result was consistent with the previous report on the magnetic liposomes containing hydrophobic iron oxide MNPs of various diameters [38]. Based on this report there is an upper limit of about 8 nm for inclusion of such MNPs within the lipid membrane. Such small MNPs upon interaction with the AC MF are undergoing Neel relaxation due to the movement of the magnetic moments relative to the crystal lattice of the nanoparticle [17]. The ability of MNPs to undergo Brown relaxation that involves movement of the particles relative to their surrounding (necessary for magneto-mechanical effects in the AC MF [17]) decreases as the diameter of the particles decreases below 8-10 nm. Despite difference in the loading and small particle size both types of MNPs used in our study produced low frequency AC MF responsive magnetic liposomes, which is promising for practical implementation of the proposed approach.

Second, we modified the structure of the liposomes by introducing a PEGylated lipid, DSPE-PEG2000, which results in the grafting of the PEG chains to the liposome membrane. PEGylation is a principal technique used in drug delivery applications to stabilize liposomes in the presence of serum, decrease elimination of liposomes by the cells of the reticuloendothelial system and increase liposome circulation time [39]. To avoid formation of micelles [40] we kept the amount of the PEGylated lipid relatively low (5 % mol. or less). At the studied compositions DSPE-PEG did not significantly affect the MNPs loading or ability of the liposomes to entrap a water-soluble dye. Both liposome types were field-responsive and accelerated the release of the dye under the AC MF. However, PEGylated liposomes appeared to be less leaky with respect to the dye both with and without the field. This result was expected, as the hydrated polymeric shell of PEG chains formed around the lipid bilayer hinders the permeability of the membranes in the PEGylated liposomes. Additionally, the non-PEGylated liposomes were nearly twice larger compared to the PEGylated ones and displayed a tendency to aggregate after application of the magnetic field. According to TEM images, non-PEGylated liposomes were nearly completely destructed after the application of the magnetic field while the PEGylated liposomes maintained some vesicle-like structures with the clustered magnetic nanoparticles embedded in them.

Finally, we modified the lipid membrane composition by introducing either Chol or unsaturated lipids. Both resulted in major changes of the behavior of magnetic liposomes under the AC MF. In particular, addition of Chol greatly diminished the release of the dye from the saturated lipid DSPC based magnetic liposomes under the field. Similarly, replacement of the DSPC for unsaturated lipid eggPC also decreased the rate of the release of the dye. The difference became more dramatic as the temperature increased from 25°C to 37°C. Notably, both studied temperatures were below the phase transition of DSPC (54-56°C) but above the phase transition of eggPC (3-4°C) as determined by the DSC (Supplementary Figure S4). In other words the membranes of the DSPC-based liposomes were in the gel phase, while eggPC liposomes were liquid crystalline. Hence, we can suggest that in order to produce optimal conditions for the field-induced release of the dye from the magnetic liposomes the lipid bilayer needs to be in the gel phase. Of particular relevance to our work is the well-known observation that the permeability of the liposomal membranes is maximal around the phase transition temperature and decreases both below and above it [41]. It is likely that the irregularities in the packaging of the lipid molecules during the phase transition facilitate the passage of small solutes across the membranes. We posit that the oscillating motion of the MNPs embedded in the gel phase membranes can more easily bring them to the disrupted irregular lipid packaging state (e.g. similar to that observed upon the phase transition) or to the rupture point. The temperature increase below the phase transition brings such bilayers closer to the brink of the most permeable state thereby facilitating “the job” of the MNPs within the membrane in the AC MF. In contrast, the more modest field-induced permeability effects in the fluid unsaturated lipid membranes may be explained by their greater ability to “heal” the deformations and defects created by the mechanical motion of the MNPs compared to the gel phase lipid bilayers. As far as the effects of Chol, the latter is known to fill the gaps between the acyl chains of the lipids resulting in the decreased permeability of the liquid crystalline bilayers [42] and enhance lateral diffusion of the gel phase bilayers [43]. Both effects appear to be consistent with the inhibitory effect of Chol on the dye release from the magnetic liposomes in the AC MF.

The liposomes used in drug delivery applications are designed to increase their stability upon storage and exposure to biological environments and decrease the leakage of the incorporated drugs. Thereby they are commonly PEGylated, and contain both saturated phospholipids and Chol. For example, PEGylated liposomal doxorubicin (PLD, also known as Doxil®) marketed in many countries as an anti-cancer drug contains hydrogenated phosphatidylcholine, Chol and DSPE-PEG (56:38:5 mol/mol) [44]. Our study enables rational design of such systems and reinforces the similar composition for the AC MF responsive magnetic liposomes albeit with a much lower content of Chol or Chol-free. Moreover, the future magnetic liposomes for remotely controlled drug delivery applications may benefit from incorporation of MNPs resulting in the decreased leakage of the lipid bilayers in the presence of the serum observed in our work. Therefore, this work advances basic knowledge and understanding of underlying phenomena of a solute release from the magnetic liposomes in AC MF and provides rationale for the design of such liposomes for future biomedical applications.

Conclusions

In this work we report the preparation and characterization of the magnetic liposomes of various lipid compositions using hydrophobized iron oxide MNPs (5 and 7 nm in diameter). The study was carried out to understand the processes leading to the release of a fluorescent dye from the magnetic liposomes, actuated by low frequency AC MF, and examine dependence of the field effect on the system's structural parameters.

ATR-FTIR spectrometry confirms perturbations in lipid bilayer structure after the exposure of the magnetic liposomes to the field. The PEGylation of the liposomes increases their stability and slightly decreases the leakage of the membrane. Addition of Chol greatly diminishes the release of the dye from the saturated lipid DSPC based magnetic liposomes under the field. Replacement of the DSPC for unsaturated lipid eggPC also decreases the rate of the release of the dye. The dye release depends on the temperature as well as the strength but not the frequency of the field. After application of the AC MF the MNPs form clusters that may enhance forces and deformations generated by the oscillating MNPs in the lipid membrane. The use of DC fields of similar strength does not release the solutes from the magnetic liposomes.

The explanation of the observed phenomena is provided according to which the oscillating motion of MNPs embedded in the gel phase lipid membranes disrupts the lipid packaging (similar to the phase transition state) increasing permeability or causing the rupture of the membrane. As the temperature increases the likelihood of such transition also increases. In the liquid crystalline membranes formed by unsaturated lipids or in Chol containing membranes the deformations and defects created by mechanical motion of the MNPs are more likely to heal. Thus, this work advances basic understanding of the processes in the magnetic liposomes in AC MF and is of significance for applied research.

Supplementary Material

Refer to Web version on PubMed Central for supplementary material.

Acknowledgements

This work was supported in parts by the National Cancer Institute (NCI), Alliance for Nanotechnology in Cancer (Carolina Center of Cancer Nanotechnology Excellence U54CA198999, pilot project to MS), the NCI (1R21CA220148 to AVK), the Eshelman Institute for Innovation (tier 2 grant to AVK) and the Russian Foundation for Basic Research (grants 1754-33027 and 18-29-09154 to NLK). We also acknowledge the Mescal S. Ferguson endowed professorship that provided in part funds for US team members travel. The authors also acknowledge Lomonosov Moscow State University Development Program PNR 5.13 (electron microscopy, ATR-FTIR, NTA).

Abbreviations

AC MF	alternating current magnetic field
MNP	magnetic nanoparticle
TEM	transmission electron microscopy
ATR-FTIR	attenuated total reflection Fourier transfer infrared

Chol	cholesterol
DSPC	1,2-Distearoyl-sn-glycero-3-phosphocholine
eggPC	egg L-α-phosphatidylcholine
DC MF	direct current magnetic field
FDA	The Food and Drug Administration
Tm	phase transition temperature
$Fe(acac)_3$	Iron (III) acetylacetonate
DMF	dimethylformamide
r.t.	room temperature
CF	carboxyfluorescein
PNDA	N-palmitoyl 6-nitro-dopamine
DI	deionized
DSPE-PEG2000	1,2-distearoyl-sn-glycero-3-phosphoethanol-amine-N-[methoxy-(polyethylene glycol)-2000] ammonium salt
PBS	phosphate-buffered saline
ICP-AES	Inductively coupled plasma atomic emission spectrometry
NTA	nanoparticles tracking analysis
DLS	dynamic light scattering
PDI	polydispersity index
AFM	atomic force microscopy
MFM	magnetic force microscopy
TGA	thermogravimetric analysis
FBS	fetal bovine serum

References

[1]. Uhrich KE, Uhrich KE, Cannizzaro SM, Cannizzaro SM, Langer RS, Langer RS, Shakesheff KM, Shakesheff KM, Polymeric systems for controlled drug release, Chem. Rev. 99 (1999) 3181–3198. doi:10.1021/cr940351u. [PubMed: 11749514]

[2]. Antipina MN, Sukhorukov GB, Remote control over guidance and release properties of composite polyelectrolyte based capsules, Adv. Drug Deliv. Rev. 63 (2011) 716–729. doi:10.1016/j.addr.2011.03.012. [PubMed: 21510987]

[3]. Han Y, Shchukin D, Yang J, Simon CR, Fuchs H, Möhwald H, Biocompatible protein nanocontainers for controlled drugs release, ACS Nano. 4 (2010) 2838–2844. doi:10.1021/nn100307j. [PubMed: 20394391]

[4]. Rösler A, Vandermeulen GWM, Klok HA, Advanced drug delivery devices via self-assembly of amphiphilic block copolymers, Adv. Drug Deliv. Rev. 64 (2012) 270–279. doi:10.1016/j.addr.2012.09.026.

[5]. Marsh D, Watts A, Knowles PF, Evidence for Phase Boundary Lipid. Permeability of Tempocholine into Dimyristoylphosphatidylcholine Vesicles at the Phase Transition, Biochemistry. 15 (1976) 3570–3578. doi:10.1021/bi00661a027. [PubMed: 182212]

[6]. Moreno MM, Garidel P, Suwalsky M, Howe J, Brandenburg K, The membrane-activity of Ibuprofen, Diclofenac, and Naproxen: A physico-chemical study with lecithin phospholipids, Biochim. Biophys. Acta - Biomembr. 1788 (2009) 1296–1303. doi:10.1016/j.bbamem.2009.01.016.

[7]. Torchilin VP, Multifunctional, stimuli-sensitive nanoparticulate systems for drug delivery, Nat. Rev. Drug Discov. 13 (2014) 813 10.1038/nrd4333. [PubMed: 25287120]

[8]. Mura S, Nicolas J, Couvreur P, Stimuli-responsive nanocarriers for drug delivery, Nat. Mater. 12 (2013) 991 10.1038/nmat3776. [PubMed: 24150417]

[9]. Viroonchatapan E, Masaharu U, Sato H, Adachi I, Nagae H, Tazawa K, Horikoshi I, Preparation and Characterization of dextran magnetite incorporated thermosensititve liposomes, Pharm. Res. 12 (1995) 1176–1183. [PubMed: 7494831]

[10]. Pradhan P, Giri J, Rieken F, Koch C, Mykhaylyk O, Döblinger M, Banerjee R, Bahadur D, Plank C, Targeted temperature sensitive magnetic liposomes for thermo-chemotherapy, J. Control. Release. 142 (2010) 108–121. doi:10.1016/j.jconrel.2009.10.002. [PubMed: 19819275]

[11]. Ding X, Cai K, Luo Z, Li J, Hu Y, Shen X, Biocompatible magnetic liposomes for temperature triggered drug delivery, Nanoscale. 4 (2012) 6289–6292. doi:10.1039/c2nr31292a. [PubMed: 22976154]

[12]. Chen Y, Chen Y, Xiao D, Bose A, Deng R, Bothun GD, Low-dose chemotherapy of hepatocellular carcinoma through triggered-release from bilayer-decorated magnetoliposomes, Colloids Surfaces B Biointerfaces. 116 (2014) 452–458. doi:10.1016/j.colsurfb.2014.01.022. [PubMed: 24549047]

[13]. Grüll H, Langereis S, Hyperthermia-triggered drug delivery from temperature-sensitive liposomes using MRI-guided high intensity focused ultrasound, J. Control. Release. 161 (2012) 317–327. doi:10.1016/j.jconrel.2012.04.041. [PubMed: 22565055]

[14]. Dai M, Wu C, Fang HM, Li L, Yan JB, Zeng DL, Zou T, Thermo-responsive magnetic liposomes for hyperthermia-triggered local drug delivery, J. Microencapsul. 34 (2017) 408–415. doi:10.1080/02652048.2017.1339738. [PubMed: 28590788]

[15]. Peiris PM, Bauer L, Toy R, Tran E, Pansky J, Doolittle E, Schmidt E, Hayden E, Mayer A, Keri R. a., Griswold M. a., Karathanasis E, Enhanced delivery of chemotherapy to tumors using a multicomponent nanochain with radio-frequency-tunable drug release, ACS Nano. 6 (2012) 4157–4168. doi:10.1021/nn300652p. [PubMed: 22486623]

[16]. Amstad E, Kohlbrecher J, Elisabeth M, Schweizer T, Textor M, Reimhult E, Triggered Release from Liposomes through Magnetic Actuation of Iron Oxide Nanoparticle Containing Membranes, (2011) 1664–1670. doi:10.1021/nl2001499.

[17]. Golovin YI, Gribanovsky SL, Golovin DY, Klyachko NL, Majouga AG, Master AM, Sokolsky M, Kabanov AV, Towards nanomedicines of the future: Remote magneto-mechanical actuation of nanomedicines by alternating magnetic fields, J. Control. Release. 219 (2015) 43–60. doi:10.1016/j.jconrel.2015.09.038. [PubMed: 26407671]

[18]. Dobson J, Remote control of cellular behaviour with magnetic nanoparticles. Nature Nanotechnology. 3 (2008) 139–143. doi:10.1038/nnano.2008.39

[19]. Klyachko NL, Sokolsky-Papkov M, Pothayee N, Efremova MV, Gulin DA, Pothayee N, Kuznetsov AA, Majouga AG, Riffle JS, Golovin YI, Kabanov AV, Changing the enzyme reaction rate in magnetic nanosuspensions by a non-heating magnetic field, Angew. Chemie - Int. Ed. 51 (2012) 12016–12019. doi:10.1002/anie.201205905.

[20]. Master AM, Williams PN, Pothayee N, Pothayee N, Zhang R, Vishwasrao HM, Golovin YI, Riffle JS, Sokolsky M, Kabanov AV, Remote actuation of magnetic nanoparticles for cancer cell selective treatment through cytoskeletal disruption, Sci. Rep. 6 (2016) 1–13. doi:10.1038/srep33560. [PubMed: 28442746]

[21]. Nappini S, Bonini M, Ridi F, Baglioni P, Structure and permeability of magnetoliposomes loaded with hydrophobic magnetic nanoparticles in the presence of a low frequency magnetic field, Soft Matter. 7 (2011) 4801–4811. doi:10.1039/c0sm01264e.

[22]. Bi H, Ma S, Li Q, Han X, Magnetically triggered drug release from biocompatible microcapsules for potential cancer therapeutics, J. Mater. Chem. B. 4 (2016) 3269–3277. doi:10.1039/c5tb02464a.

[23]. Qiu D, An X, Controllable release from magnetoliposomes by magnetic stimulation and thermal stimulation, Colloids Surfaces B Biointerfaces. 104 (2013) 326–329. doi:10.1016/j.colsurfb.2012.11.033. [PubMed: 23290769]

[24]. Guo H, Chen W, Sun X, Liu YN, Li J, Wang J, Theranostic magnetoliposomes coated by carboxymethyl dextran with controlled release by low-frequency alternating magnetic field, Carbohydr. Polym. 118 (2015) 209–217. doi:10.1016/j.carbpol.2014.10.076. [PubMed: 25542126]

[25]. Golovin Y, Golovin D, Klyachko N, Majouga A, Kabanov A, Modeling drug release from functionalized magnetic nanoparticles actuated by non-heating low frequency magnetic field, J. Nanoparticle Res. 19 (2017). doi:10.1007/s11051-017-3754-5.

[26]. Vishwasrao HM, Master AM, Seo YG, Liu XM, Pothayee N, Zhou Z, Yuan D, Boska MD, Bronich TK, Davis RM, Riffle JS, Sokolsky-Papkov M, Kabanov AV, Luteinizing Hormone Releasing Hormone-Targeted Cisplatin-Loaded Magnetite Nanoclusters for Simultaneous MR Imaging and Chemotherapy of Ovarian Cancer, Chem. Mater. 28 (2016) 3024–3040. doi:10.1021/acs.chemmater.6b00197.

[27]. Joniec A, Sek S, Krysinski P, Magnetoliposomes as Potential Carriers of Doxorubicin to Tumours, Chem. - A Eur. J. 22 (2016) 17715–17724. doi:10.1002/chem.201602809.

[28]. Bensikaddour H, Snoussi K, Lins L, Van Bambeke F, Tulkens PM, Brasseur R, Goormaghtigh E, Mingeot-Leclercq MP, Interactions of ciprofloxacin with DPPC and DPPG: Fluorescence anisotropy, ATR-FTIR and 31P NMR spectroscopies and conformational analysis, Biochim. Biophys. Acta - Biomembr. 1778 (2008) 2535–2543. doi:10.1016/j.bbamem.2008.08.015.

[29]. Moreno MM, Garidel P, Suwalsky M, Howe J, Brandenburg K, The membrane-activity of Ibuprofen, Diclofenac, and Naproxen: A physico-chemical study with lecithin phospholipids, Biochim. Biophys. Acta - Biomembr. 1788 (2009) 1296–1303. doi:10.1016/j.bbamem.2009.01.016.

[30]. Mirosavljevi K, Noethig-laslo V, Effects of Cholesterol Concentrations on Egg-phosphatidylcholine – Dihexadecyl-phosphate Liposomes Studied by CW ESR and FT – ESEEM Spectroscopy, 81 (2008) 631–636.

[31]. Nappini S, Bonini M, Bombelli F, Pineider F, Sangregorio C, Baglioni P, Nordén P,&B, Controlled drug release under a low frequency magnetic field: effect of the citrate coating on magnetoliposomes stability. Soft Matter, 7 (2011) 1025–1037. doi:10.1039/c0sm00789g

[32]. Shirmardi Shaghasemi B, Virk MM, Reimhult E, Optimization of Magneto-thermally Controlled Release Kinetics by Tuning of Magnetoliposome Composition and Structure, Sci. Rep. 7 (2017) 1–10. doi:10.1038/s41598-017-06980-9. [PubMed: 28127051]

[33]. Chen Y, Bose A, Bothun GD, Controlled release from bilayer-decorated magnetoliposomes via electromagnetic heating, ACS Nano. 4 (2010) 3215–3221. doi:10.1021/nn100274v. [PubMed: 20507153]

[34]. Spera R, Apollonio F, Liberti M, Paffi A, Merla C, Pinto R, & Petralito S, Controllable release from high-transition temperature magnetoliposomes by low-level magnetic stimulation. Colloids and Surfaces B: Biointerfaces, 131 (2015) 136–140. doi:10.1016/j.colsurfb.2015.04.030 [PubMed: 26042528]

[35]. Jia B, & Gao L, Morphological Transformation of Fe_3O_4 Spherical Aggregates from Solid to Hollow and Their Self-Assembly under an External Magnetic Field. The Journal of Physical Chemistry C, 112 (2008) 666–671. doi:10.1021/jp0763477

[36]. Saville SL, Qi B, Baker J, Stone R, Camley RE, Livesey KL, Thompson Mefford O, The formation of linear aggregates in magnetic hyperthermia: Implications on specific absorption rate and magnetic anisotropy. Journal of Colloid and Interface Science, 424 (2014) 141–151. doi:10.1016/j.jcis.2014.03.007. [PubMed: 24767510]

[37]. Jin R, Lin B, Li D & Ai H, Superparamagnetic iron oxide nanoparticles for MR imaging and therapy: design considerations and clinical applications. Current Opinion in Pharmacology, 18 (2014) 18–27. doi:10.1016/j.coph.2014.08.002. [PubMed: 25173782]

[38]. Michel R, Gradzielski M, Experimental Aspects of Colloidal Interactions in Mixed systems of liposome and inorganic nanoparticle and their applications, Int. J. Mol. Sci. 13 (2012) 11610–11642. doi:10.3390/ijms130911610. [PubMed: 23109874]

[39]. Torchilin VP, Recent advances with liposomes as pharmaceutical carriers, Nat. Rev. Drug Discov. 4 (2005) 145–160. doi:10.1038/nrd1632. [PubMed: 15688077]

[40]. Abe K, Higashi K, Watabe K, Kobayashi A, Limwikrant W, Yamamoto K, Moribe K, Effects of the PEG molecular weight of a PEG-lipid and cholesterol on PEG chain flexibility on liposome surfaces, Colloids Surfaces A Physicochem. Eng. Asp. 474 (2015) 63–70. doi:10.1016/j.colsurfa.2015.03.006.

[41]. Demel RA, Kinsky SC, Kinsky CB, & Van Deenen LLM, Effects of temperature and cholesterol on the glucose permeability of liposomes prepared with natural and synthetic lecithins. Biochimica et Biophysica Acta (BBA) - Biomembranes, 150 (1968) 655–665. doi:10.1016/0005-2736(68)90055-2. [PubMed: 5660373]

[42]. Hung W-C, Lee M-T, Chen F-Y, & Huang HW, The Condensing Effect of Cholesterol in Lipid Bilayers. Biophysical Journal, 92 (2007) 3960–3967. doi:10.1529/biophysj.106.099234. [PubMed: 17369407]

[43]. Wu E, Jacobson K, Papahadjopoulos D, Lateral diffusion in phospholipid multibilayers measured by fluorescence recovery after photobleaching. Biochemistry, 16 (1977) 3936–3941. doi:10.1021/bi00636a034. [PubMed: 901758]

[44]. Gabizon A, Shmeeda H, Barenholz Y, Pharmacokinetics of Pegylated Liposomal Doxorubicin. Clinical Pharmacokinetics, 42 (2003) 419–436. doi:10.2165/00003088-200342050-00002. [PubMed: 12739982]

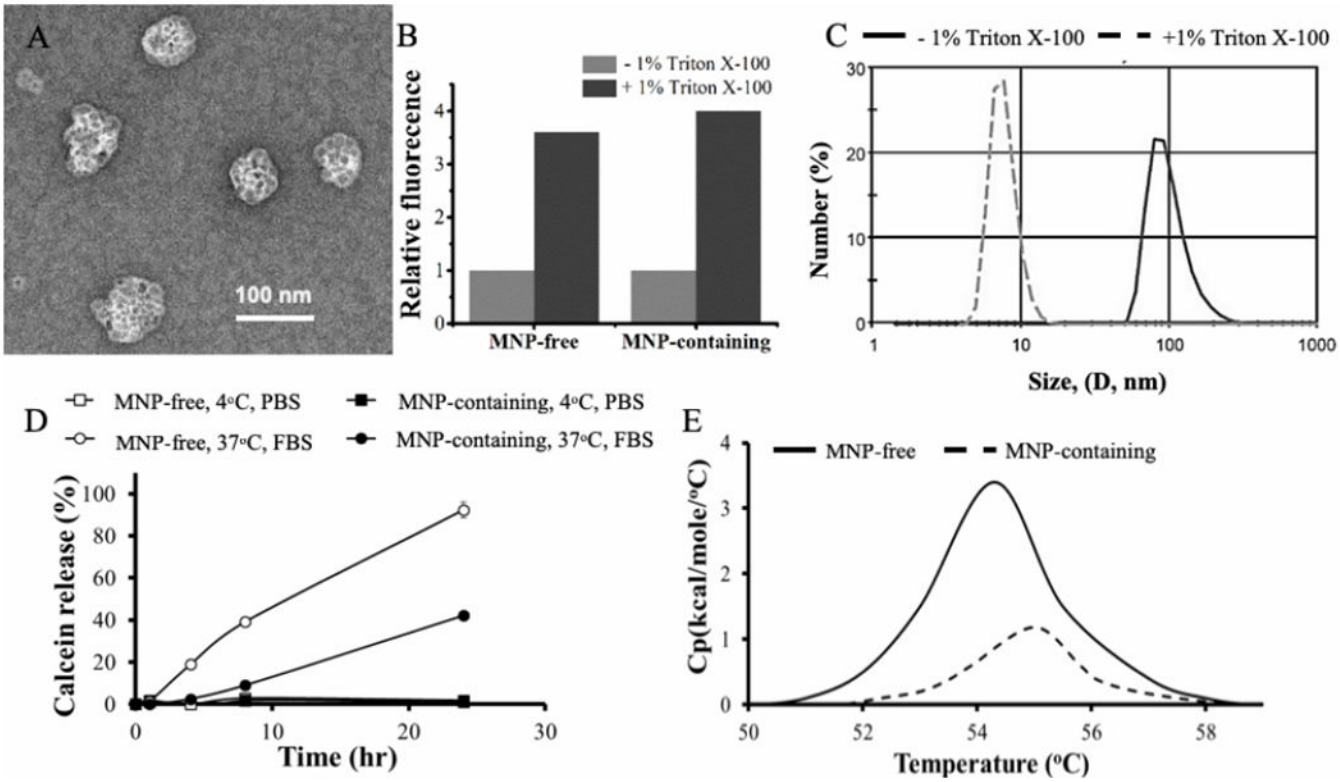

Figure 1.

Physicochemical characterization of MNP-free and MNP-containing DSPC/DSPE-PEG2000 (95:5) liposomes (LPS and M-LPS, respectively). (**A**) TEM of MNP-containing liposomes, (**B**) calcein release following treatment of liposomes with 1% Triton X-100, (**C**) DLS of MNP-containing liposomes, (**D**) Stability of liposomes at 4°C in PBS and 37°C in FBS/PBS as measured by calcein release, (**E**) DSC of MNP-free and MNP-containing liposomes. All MNP-liposomes contain 5.5 % wt. PNDA-coated 5 nm MNP. The concentration of lipids was 0.08 mg lipid/ml.

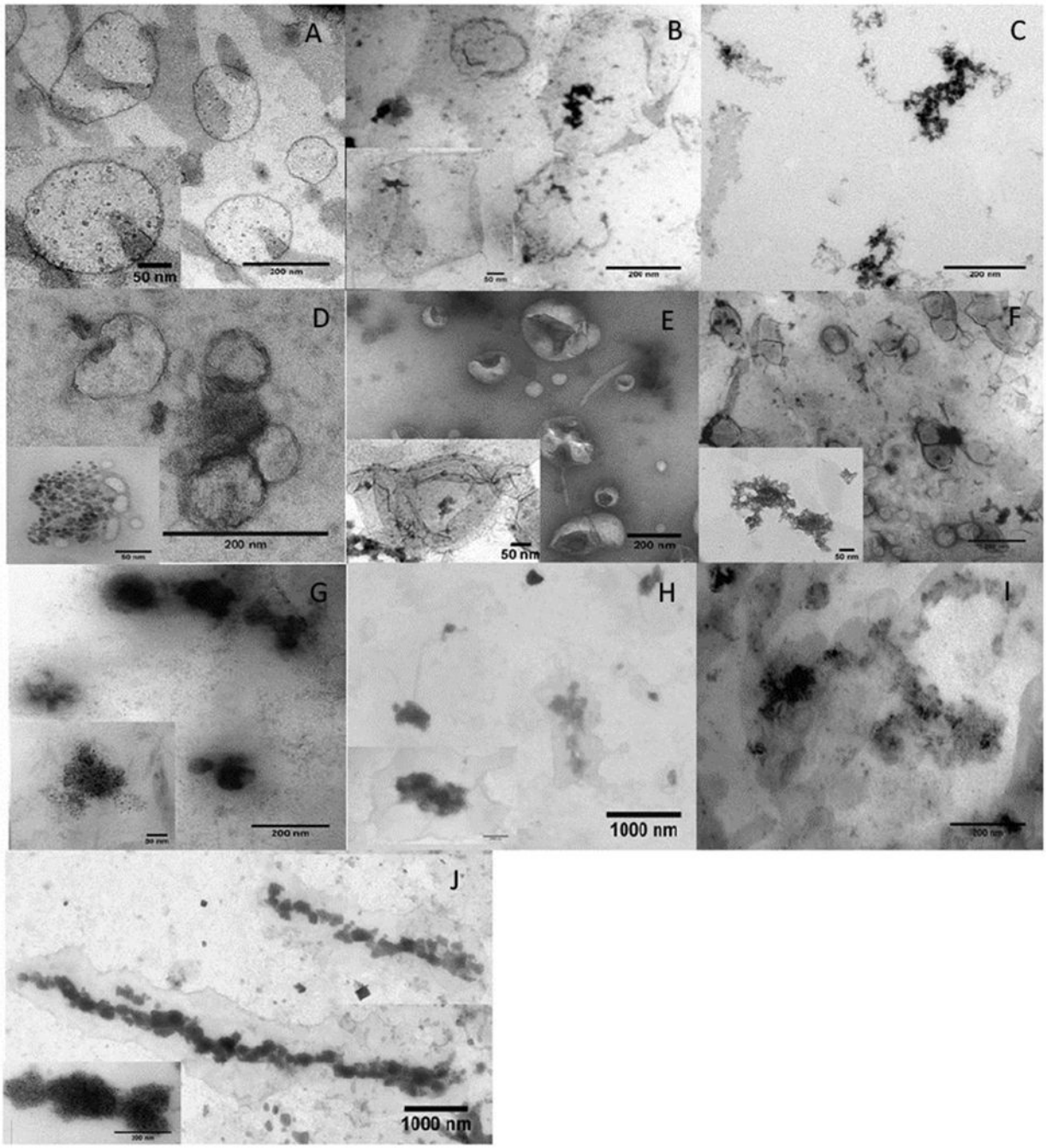

Figure 2.

TEM images of MNP-containing liposomes (**A, D, G**) before and after exposure to AC MF (50 Hz 50 kA/m) for different duration: (**B, E, H**) 5 min; (**C, F, I**) 25 min. Liposome composition: (**A-C**) eggPC/Chol (85:15 mol/mol) containing 0.8% wt. eggPC-coated 7 nm MNP; (**D-F**) eggPC/Chol/DSPE-PEG (81:4:15 mol/mol) containing 1.2% wt. eggPC-coated 7 nm MNP; (**G-J**) eggPC/Chol/DSPE-PEG (81:4:15 mol/mol) containing 1.8 % wt. eggPC-coated 5 nm MNP. (**J**) MNP-containing liposomes after 5 min exposure to DC MF (57 kA/m) at 25°C. (**A-J**) Liposome concentration during exposure was 0.012 mg lipid/ml.

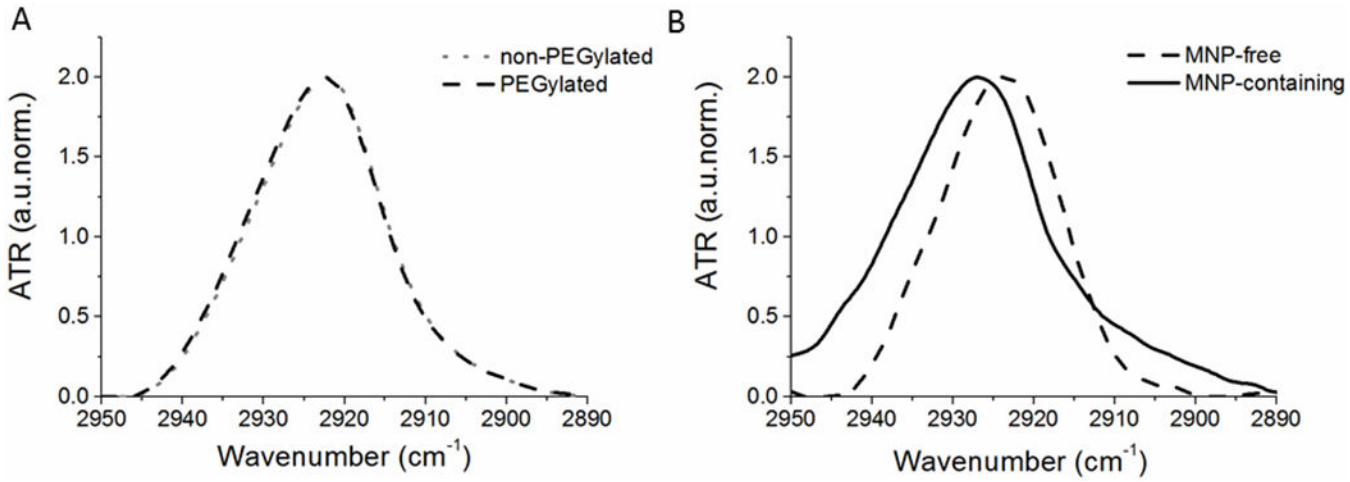

Figure 3.

The absorption bands corresponding to asymmetric oscillations of CH_2 groups of (**A**) MNP-free non-PEGylated and PEGylated liposomes and (**B**) MNP-free and MNP-containing PEGylated liposomes. Liposome composition: eggPC/Chol (85:15 mol/mol); eggPC/DSPE-PEG2000/Chol (81:4:15 mol/mol); or eggPC/DSPE-PEG2000/Chol (81:4:15 mol/mol) containing 1.8% wt. eggPC-coated 5 nm MNP. Liposome concentration was 12 mg lipid/ml in 10 mM PBS (pH=7.4) at 22°C.

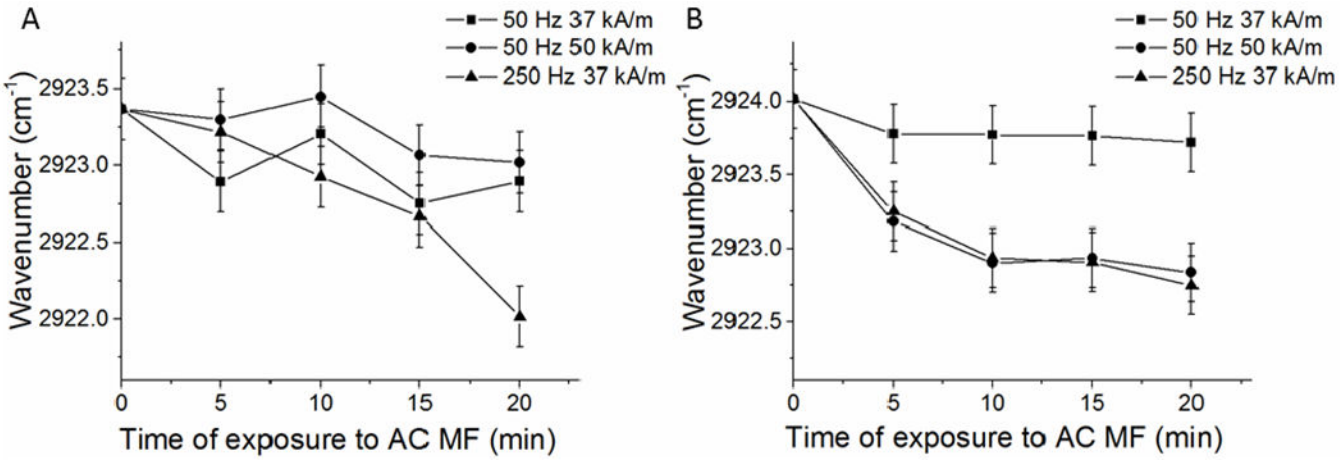

Figure 4.

Changes in the absorption band of asymmetric oscillations of CH_2 groups of (**A**) non-PEGylated and (**B**) PEGylated magnetic liposomes after exposures to AC MF. Liposome composition: (**A**) eggPC/Chol (85:15 mol/mol) containing 1% wt. eggPC-coated MNP (5 nm); or (**B**) eggPC/DSPE-PEG2000/Chol (81:4:15 mol/mol) containing 1.8% wt. eggPC-coated 5 nm MNP. Liposome concentration 12 mg lipid/ml in 10 mM PBS, pH=7.4. Exposure to AC MF was carried out at r.t.. Error bars correspond to the precision of the peak position measurement (±0.2 cm^{-1}).

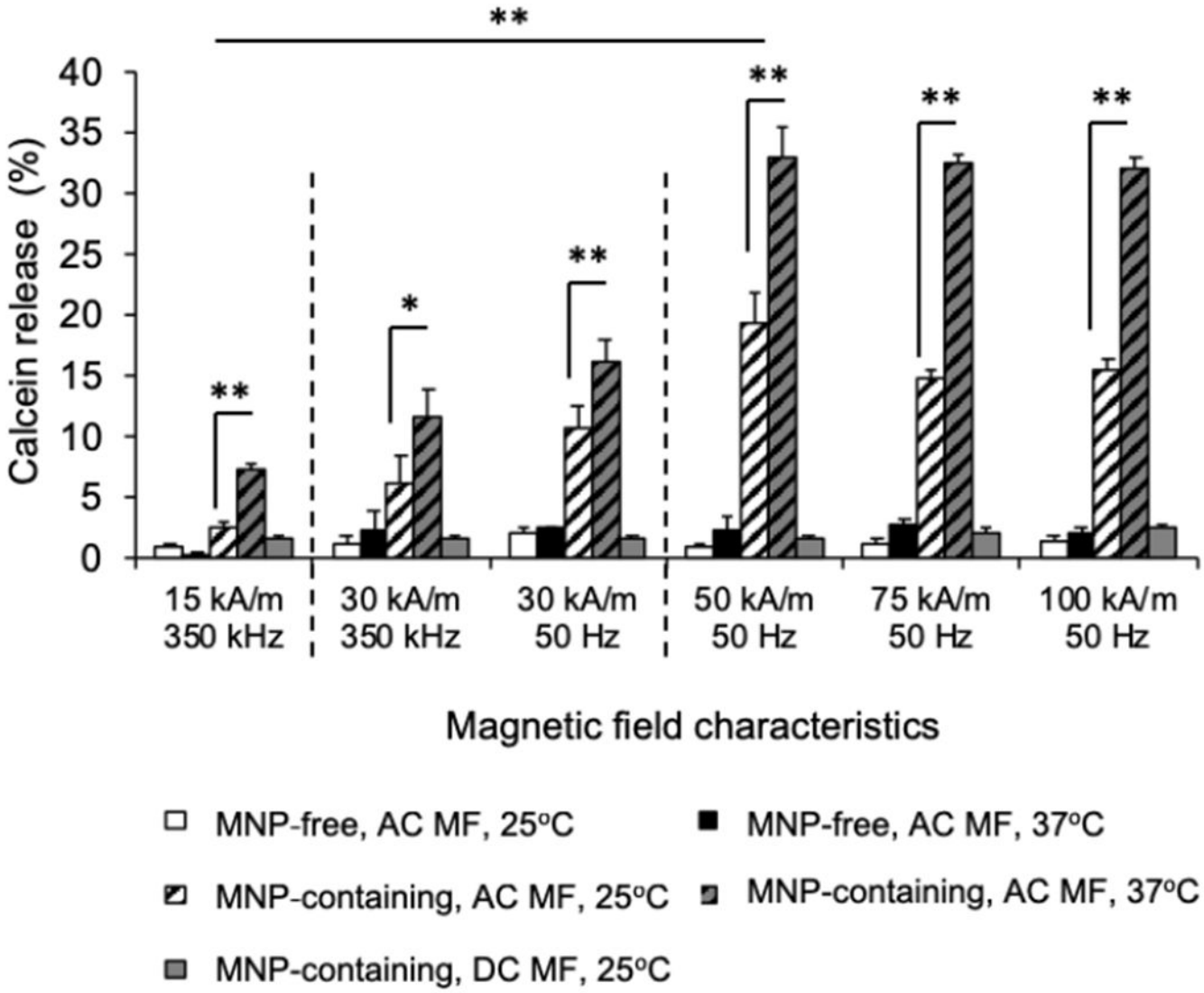

Figure 5.

Effect of AC MF strength and frequency and environmental temperature on calcein release from MNP-free and MNP-containing DSPC/DSPE-pEg2000 (95:5) liposomes (LPS and M-LPS, respectively). MNP-liposomes contain 5.5 % wt. PNDA-coated 5 nm MNP. Liposome dispersions were prepared at 0.16 mg lipid/ml and exposed to AC MF of specified field strength/frequency or DC magnetic field of the equivalent strength for 30 min. *p=0.03, ** p<0.01 (n = 3).

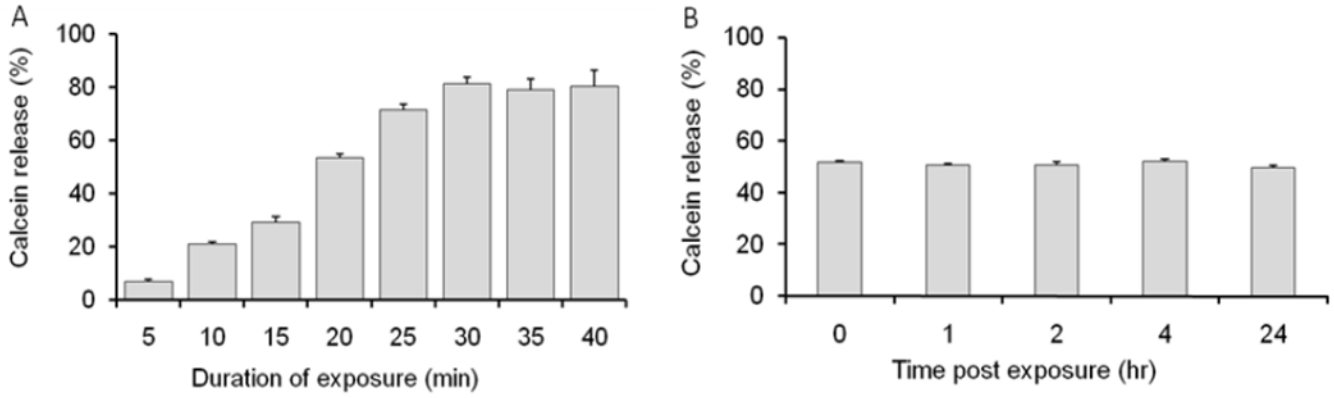

Figure 6.

Kinetics of calcein release from magnetic liposomes exposed to AC MF (50 kA/m, 50 Hz) at 37°C. (**A**) Calcein release as the function of time of exposure and (**B**) calcein release at different times after 20 min exposure to the field. Liposome composition: DSPC/DSPE-PEG2000 (95:5) containing 5.5 % wt. PNDA-coated 5 nm MNP. Liposome concentration: 0.08 mg lipid/ml. (n=3).

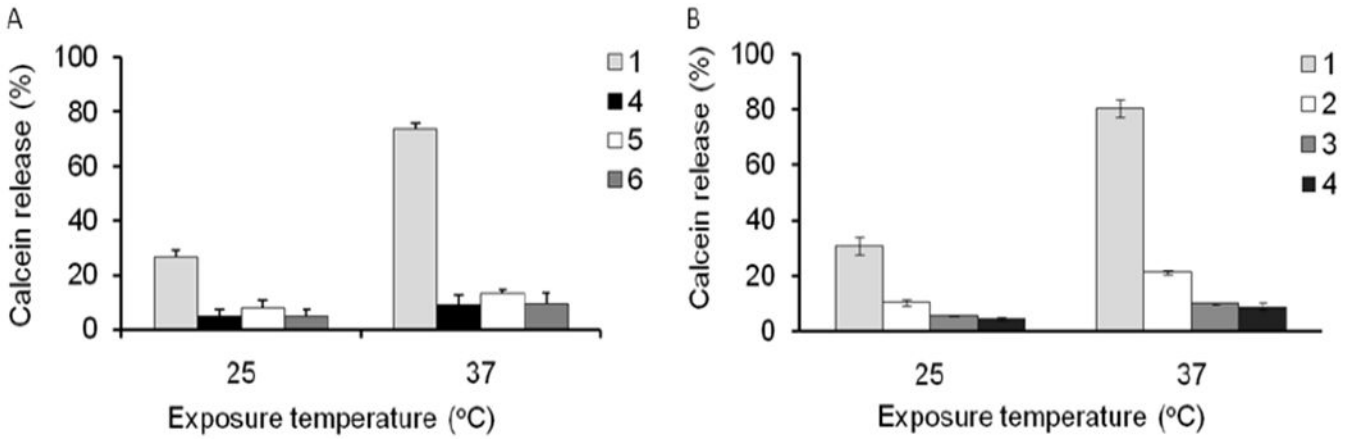

Figure 7.

Effect of (**A**) lipid saturation and (**B**) cholesterol content on the field-induced release of calcein from magnetic liposomes containing PNDA-coated 5 nm MNP. Liposome composition (1) DSPC/DSPE-PEG2000 (95:5), (2) DSPC/DSPE-PEG2000/Chol (75.9:3.8:20.3), (3) DSPC/DSPE-PEG2000/Chol (0.6:3.0:36.4), (4) DSPC/DSPE-PEG2000/Chol (48.0:2.4:49.6), (5) eggPC/DSPE-PEG2000 (95:5) and (6) eggPC/DSPE-PEG2000/Chol (49.2:2.6:48.2). The liposomes contained PNDA-coated 5 nm MNP: (1) 5.5%, (2) 9.6%, (3) 8.8%, (4) 5.7%, (5) 8.9% and (6) 9%. The samples were exposed to AC MF (50kA/m and 50Hz) at 25°C and 37°C for 30 min. Liposome concentration: 0.018 mg lipid/ml. (n=3).

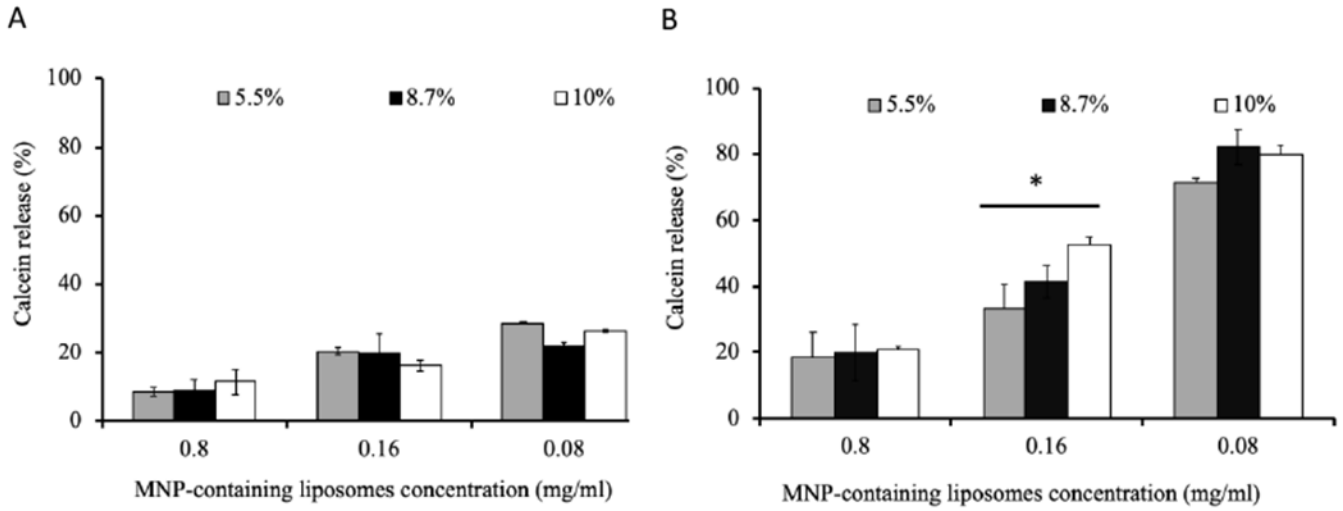

Figure 8.

Effect of sample concentration and MNP content on the calcein release from magnetic liposomes exposed to AC MF. Liposome composition: DSPC/DSPE-PEG2000 (95:5) containing 5.5%, 8.7% or 10% wt. PNDA-coated 5 nm MNP. Liposomes were exposed for 30 min to AC MF (50 kA/m, 50 Hz) at (**A**) 25°C and (**B**) 37°C. * $p<0.05$ ($n = 3$).

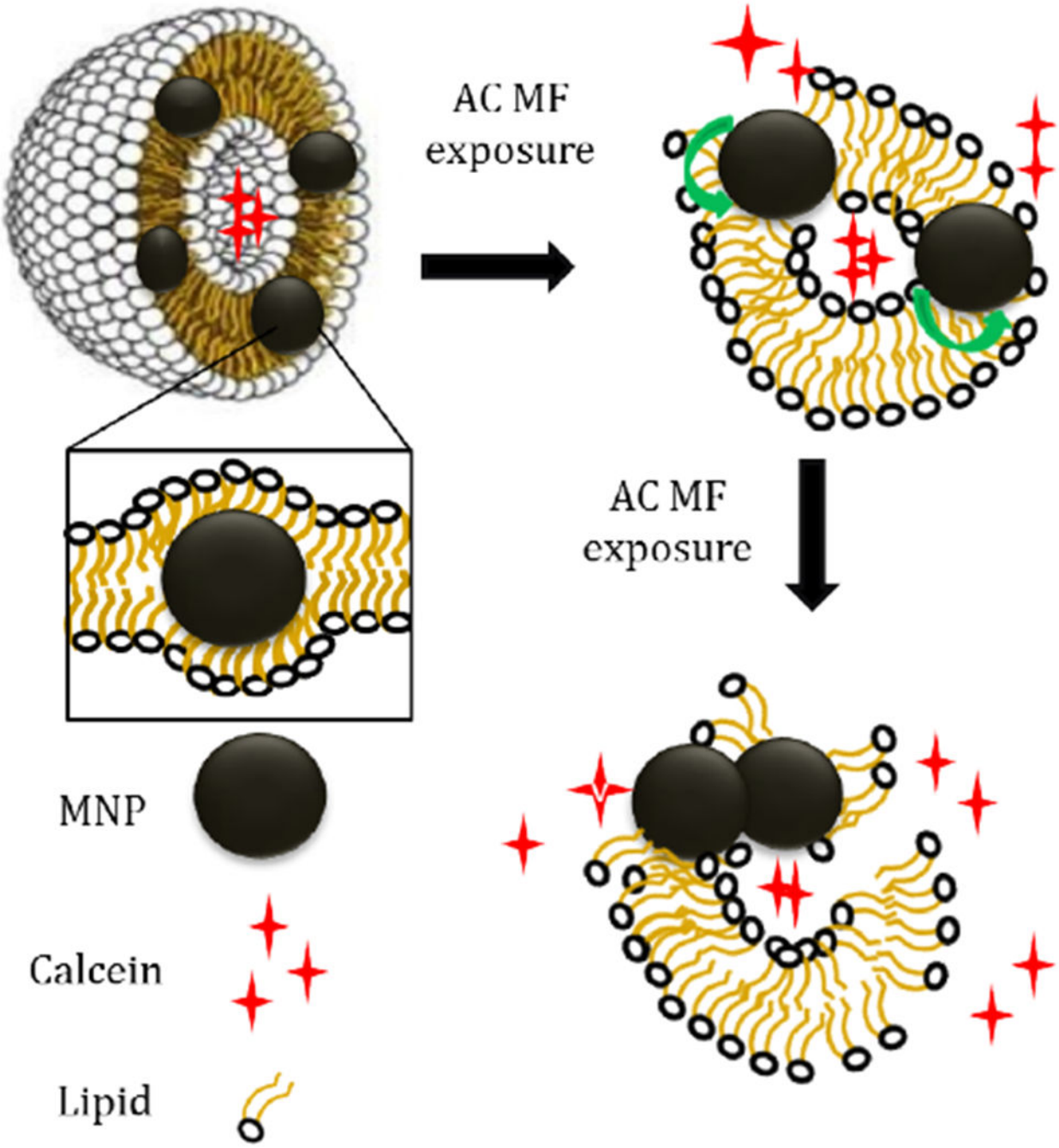

Scheme 1.
Possible mechanism of calcein release from magnetic liposomes under exposure to low frequency AC MF.

Table 1.

Composition and DLS characteristics of MNP-containing liposomes used in this work.

Lipid composition	Lipids ratio mol/mol	MNP size, coating	MNPs content, % wt.[a]	Particles diameter, D_{eff}, nm[b]	PDI[b]	ζ-Potential, mV[b]
DSPC/DSPE-PEG2000	95:5	-	-	159.±5.7	0.25±0.03	−4.7
DSPC/DSPE-PEG2000	95:5	5 nm, PNDA	5.5 [c,e]	103.7 ± 0.6	0.13 ± 0.01	− 3.2
DSPC/DSPE-PEG2000	95:5	5 nm, PNDA	8.7 [c]	100.2 ± 1.2	0.11 ± 0.03	− 3.3
DSPC/DSPE-PEG2000	95:5	5 nm, PNDA	10.0 [c]	104.5 ± 2.1	0.14 ± 0.02	− 4.2
DSPC/DSPE-PEG2000/Chol	75.9:3.8:20.3	-	-	166.±3.9	0.04±0.01	−3.8
DSPC/DSPE-PEG2000/Chol	75.9:3.8:20.3	5 nm, PNDA	9.6	102.9 ± 1.7	0.19±0.01	− 4.3
DSPC/DSPE-PEG2000/Chol	60.6:3.0:36.4	5 nm, PNDA	8.8	101.6 ± 0.4	0.11±0.018	− 4.0
DSPC/DSPE-PEG2000/Chol	48.0:2.4:49.6	5 nm, PNDA	5.7	103.7 ± 0.6	0.14 ± 0.02	− 3.2
eggPC/DSPE-PEG2000	95:5	5 nm, PNDA	8.9	100.2 ± 1.2	0.14 ± 0.01	− 3.3
eggPC/DSPE-PEG2000/Chol	49.2:2.6:48.2	5 nm, PNDA	9.0	104.5 ± 2.1	0.13 ± 0.02	− 4.2
eggPC/Chol	85:15	5 nm, eggPC [d]	1.0	150 ± 20	0.20 ± 0.10	− 12.7 ± 3.0
eggPC/DSPE-PEG2000/Chol	81:4:15	5 nm, eggPC [d]	1.8	105 ± 10	0.18 ± 0.01	− 2.4 ± 6.0
eggPC/Chol	85:15	7 nm, eggPC [d]	0.8	181 ± 3	0.21 ± 0.03	− 18.8 ± 0.5
eggPC/DSPE-PEG2000/Chol	81:4:15	7 nm, eggPC [d]	1.2	140 ± 3	0.23 ± 0.01	− 8.8 ± 0.5

[a] MNPs and lipid content in liposomes was determined by ICP-MS (unless stated differently) and expressed % wt. as MNP/(MNP+lipids) × 100%;

[b] as determined by DLS. Data are presented as mean ± SD (n=3);

[c] MNPs content in the liposomes was varied by changing the lipids/MNP ratio as presented in Supplementary Table S1;

[d] MNPs content was determined by ICP-AES and lipid content was assumed to be 100% of what was taken for liposome preparation. MNPs dispersed in eggPC in chloroform become coated by the lipid as determined by IR-spectroscopy (Supplementary Figure S5).

[e] Two separate sample preparations.

Table 2.

Changes in the particle size of magnetic liposomes, before and after exposure to AC MF as measured by DLS.

Sample composition	Temperature, °C	Before treatment		After treatment	
		D_{eff}, nm	PDI	D_{eff}, nm	PDI
DSPC/DSPE-PEG2000 (95:5)[a]	25	92 ± 3	0.22 ± 0.02	101 ± 5	0.26 ± 0.04
	37	99 ± 3	0.29 ± 0.03	105 ± 1	0.26 ± 0.01
eggPC/Chol (85:15)[b]	25	181 ± 3	0.21 ± 0.03	228 ± 10	0.40 ± 0.01
eggPC/DSPE-PEG2000/Chol (81:4:15)[c]	25	140 ± 3	0.23 ± 0.03	150 ± 10	0.25 ± 0.01
eggPC/DSPE-PEG2000/Chol (81:4:15)[d]	25	104± 1	0.18± 0.01	109± 2	0.19± 0.02

[a] Liposomes contain 10% wt. PNDA-coated MNP (5 nm); 0.08 mg lipid/ml; treatment 50 kA/m, 50 Hz, 30 min.

[b] Liposomes contain 0.8% wt. eggPC-coated MNP (7 nm); 0.12 mg lipid/ml; treatment 50 kA/m, 50 Hz, 10 min.

[c] Liposomes contain 1.2% wt. eggPC-coated MNP (7 nm); 0.12 mg lipid/ml; treatment 50 kA/m, 50 Hz, 10 min.

[d] Liposomes contain 1.8% wt. eggPC-coated MNP (5 nm); 0.12 mg lipid/ml; treatment 50 kA/m, 50 Hz, 10 min.